

## Strength And Fatigue Of Multilayer Conveyor Belts Under Cyclic Loads

<sup>1</sup>DSc., prof. R. Tojiyev, <sup>2</sup>PhD. A.Isomidinov, <sup>3</sup>Assistant. B.Alizafarov,

<sup>1</sup>Fergana Polytechnic Institute

<sup>2</sup>Fergana Polytechnic Institute

<sup>3</sup>Fergana Polytechnic Institute

Republic of Uzbekistan

e-mail:isomiddinov1985@mail.ru

---

**Annotation.:** The article states that in a multi-layer conveyor belt operating under bending, stretching conditions and when transmitting a circumferential force from the drum, a complex stress state arises, which, using the positions of the theory of elasticity, is composed of systems of integral equations describing these states.

Solutions of system of integral equations at different values of diameters of drums, modulus of elasticity, modulus of rubber shear, thickness of gaskets, interlayers and number of gaskets are obtained regularities of change of tensile stresses and shear stresses from calculated factors.

The pattern of distribution of tensile stresses between the tape gaskets under the combined action of stretching, bending and circumferential force is plotted. It follows from the graph that the tensile stresses between the gaskets are distributed unevenly, compressive stresses arise in the rubber interlayers, caused by the action of the overlying stretched gaskets on the underlying ones. The compression stresses combined with the shear stress cause constant fatigue failure of the interlayers under belt operating conditions especially at small drum diameters and high belt tension.

Also, experimental studies were required to test the analytical description.

A series of experiments were carried out under various loading conditions, the tests consisted in experiments on specific values and regular wear of the resistance of the conveyor belts under the studied conditions of interaction of the belt with the drums, bending and shifting. An experimental study confirmed that the traction force transmitted to the belt from the drive drum significantly affects its wear resistance. With increasing traction force, the number of loading cycles to fatigue fracture of the belt decreases.

A link is established between the value of variable stresses in the conveyor belt and its fatigue failure.

Methods for calculating conveyor endurance belts and practical recommendations for applying the results of the study have been developed.

---

**Key words:** gasket, interlayer, module, shear, elasticity, rubber, diameter, drum, forces, fatigue, load, strength, multilayer, bending, deformation, stresses, fabric, stretches, layer, iteration, collocation, interpolation, conveyor, friction, drum, roller.

---

### Introductions

With the growth of cargo flows and the need to design powerful long conveyors with an expensive belt, it is desirable to have a more accurate method of calculating the belt, which could take into account the phenomena arising during its operation.

Based on the analysis of the previous studies, there are a number of robots in which an attempt is made to accurately determine the individual components of the safety factor, taking into account the uneven distribution of load between the gaskets during tension [1], bending on the drums and rollers [2], dynamic overloads during start-up [3], fatigue phenomena during impact loads [4].

At the same time, we can conclude that it is necessary to develop better methods in which more factors are taken into account than so far.

In this connection, it can be recalled that it is assumed that there is no influence of normal compressive stresses between the layers of the belt moving along the drum [2]. In other works [5,6], the conclusions of the theory of composite rods are used, but rods are not considered as complex, statically undefined elements.

Despite the rigidity of the approach to the problem and the depth of study [5,6], these theories give enough simple solutions for practical application for beams, rods and packages made up of 2-3 elements and in addition solve more direct problems where deformations and stresses are sought according to given external loads.

### Theoretical study of stress.

The above circumstances forced to perform an independent analysis using the positions of the theory of elasticity. To solve the problem, the following simplifications are adopted:

- the task to consider in conditions of flat stress state, i.e. to consider stresses on the sites parallel to the plane equal to zero;
- material of fabric gaskets and rubber interlayers shall be considered subject to Hooke's law [7];
- each layer is represented by a model of extensible thread, which does not resist bending, the change in its thickness during deformation is neglected;
- the thickness of the layer, the thickness of the adhesive interlayer and the thickness of the tape are small compared to the length of the contact zone;
- we consider the problem in quasi-static staging, at low running speeds.

When the multi-layer belt runs around the drum, the stress state of the latter is caused by the initial tension of the belt, the bending of the belt around the drum ("clean" bend of the belt) and the transfer of the circumferential force.

The first type of stress state is with uniform stretching by force  $T_0$ .

With  $n + 1$  layers, the tensile force of each layer is equal. There are no tangent stresses.

Consider the "clean" bend of the tape. To find tangent stresses between the layers, split the tape into separate layers and apply them to the drum (Figure 1).

Ends of belt form steps with pitch  $h \alpha$  (1),

where  $2\alpha$  is the girth angle. We apply some normal stresses to the line (they are insignificant) and to the cut lines  $l$  tangents, which must align the points separated by the curvature of individual layers. The normal stresses appearing in the same way will not enter the equations due to paragraph 4 of the initial prerequisites.

Consider the  $K$  layer in the primary and secondary states (Figure 2). In the basic state, it is affected by the voltages  $\tau_{k-1}(x)$  and  $\tau_k(x)$ . The move will be  $V_{k-1}(x)$  and  $V_k(x)$  - unknown functions. Move the edges along the layer denote In the auxiliary state we apply a unit force on top of the layer at point  $t$ . The movement function (1) is written in the form:

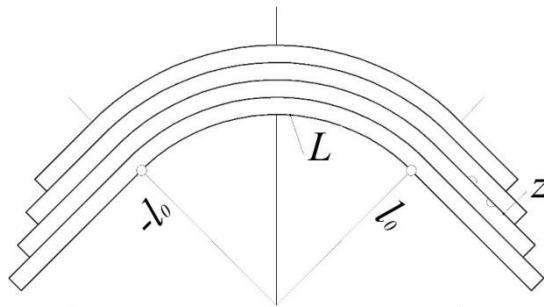


Fig. 2. Exploded multilayer ribbon

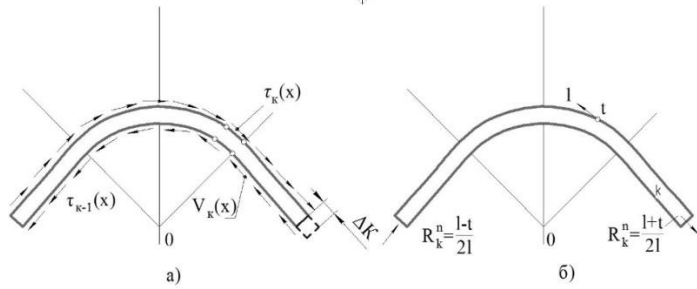


Fig. 2. Design states of the tape:  
a - main, b - auxiliary.

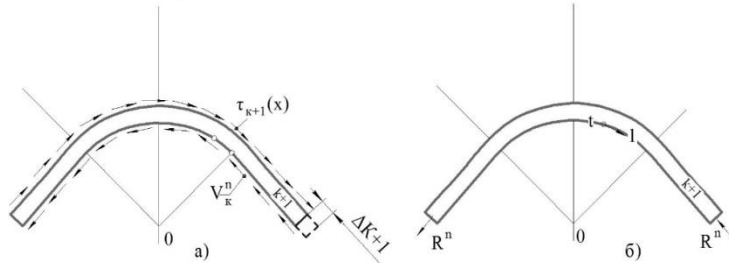


Fig. 3. Design states of the tape:  
a - main, b - auxiliary.

$$U(t, x) = k\delta(t - x) + \frac{1}{2EFt} F(t, x) \quad (1)$$

$F(t, x)$  is defined by formula (2).

Using the reciprocity theorem of work, we get the relations: for layer  $K$

$$-\frac{1}{2EFt} \int_{-t}^t \tau_{k-1}(x)F(t, x)dx + k\tau_k(t) + \frac{1}{2EFt} \int_{-t}^t \tau_k(x)F(t, x), dx = V_k^1(t) + \Delta_k (R^n - R^n) \quad (2)$$

для K+1 слоя (рис.3)

$$k\tau_k(t) + \frac{1}{2EFt} \int_{-t}^t \tau_k(x)F(t, x)dx - \frac{1}{2EFt} \int_{-t}^t \tau_{k+1}(x)F(t, x), dx = V_k^n(t) - \Delta_{k+1}(R^n - R^n). \quad (3)$$

Сложим (2) и (3)

$$2k\tau_k(x) + \frac{1}{EFt} \int_{-t}^t \tau_k(x)F(t, x), dx - \frac{1}{2EFt} \int_{-t}^t \tau_{k+1}(x)F(t, x)dx = V_k^n - V_k^1 + (\Delta_k + \Delta_{k+1})(R^n - R^n) \quad (4)$$

From this you can see that - the geometric mismatch of points in the dissected K and K + 1 layers - the step between the layers (1).

Therefore, the right side of the equation is

$$f(t) = V_k^n - V_k^1 + (\Delta_k - \Delta_{k+1})(R^n - R^n) = \begin{cases} \frac{ht}{R} - \frac{h_0 t}{R} - n\mu - t_0 \leq t \leq t_0 \\ \frac{h_0}{R} \text{Sign}t - \frac{h_0 t}{R} - n\mu(t) \geq t_0 \end{cases}$$

Thus, the equation for the joint of K and K + 1 layers has the form:

$$-\frac{\lambda}{2} \int_{-t}^t \tau_{k+1}(x)F(t, x)dx + \tau_k(t) + \lambda \int_{-t}^t \tau_k(x)F(t, x)dx - \frac{\lambda}{2} \int_{-t}^t \tau_{k+1}(x)F(t, x)dx = f(t) \frac{G}{h} \quad (5)$$

K=1, 2, 3 .....n.

With K = 1, it should be assumed that the equation contains only two integral terms; with K = n, it should be assumed that the equations will also have two integral terms.

Thus, the system is complete (i.e., the number of unknown functions is equal to the number of equations):

$$\begin{cases} \tau_1(t) + \lambda \int_{-t}^t \tau_1(x)F(t, x)dx - \frac{\lambda}{2} \int_{-t}^t \tau_2(x)F(t, x)dx = f(t) \frac{G}{h}; \\ -\frac{\lambda}{2} \int_{-t}^t \tau_1(x)F(t, x)dx + \tau_2(t) + \lambda \int_{-t}^t \tau_2(x)F(t, x)dx - \frac{\lambda}{2} \int_{-t}^t \tau_3(x)F(t, x)dx = f(t) \frac{G}{h}; \\ -\frac{\lambda}{2} \int_{-t}^t \tau_{k-1}(x)F(t, x)dx + \tau_k(t) + \lambda \int_{-t}^t \tau_k(x)F(t, x)dx - \frac{\lambda}{2} \int_{-t}^t \tau_{k+1}(x)F(t, x)dx = f(t) \frac{G}{h}; \\ -\frac{\lambda}{2} \int_{-t}^t \tau_{n-1}(x)F(t, x)dx + \tau_n(t) + \lambda \int_{-t}^t \tau_n(x)F(t, x)dx = f(t) \frac{G}{h}. \end{cases} \quad (6)$$

When transmitting the circumferential force, the system of resolving equations retains its form (6). Only  $\tau_k$  is an unknown function.

To solve the problem (6), it is necessary to supplement the equilibrium equations for each of the layers, after which the system has the only solution where Pn is the normal pressure on the tape, f is the coefficient of friction.

The system of integral equations in the transmission of the circumferential force has the form  $f(t) = 0$ :

$$\left\{ \begin{aligned} &\tau_0(t) + \lambda \int_{-t}^t \tau_0(x) F(t, x) dx - \lambda \int_{-t}^t \tau_1(x) F(t, x) dx - V_0(t) = 0; \\ &-\frac{\lambda}{2} \int_{-t}^{t_0} \tau_0(x) F(t, x) dx + \tau_1(t) + \lambda \int_{-t}^t \tau_1(x) F(t, x) dx - \frac{\lambda}{2} \int_{-t}^t \tau_2(x) F(t, x) dx = 0; \\ &-\frac{\lambda}{2} \int_{-t}^t \tau_1(x) F(t, x) dx + \tau_2(t) + \lambda \int_{-t}^t \tau_2(x) F(t, x) dx - \frac{\lambda}{2} \int_{-t}^t \tau_3(x) F(t, x) dx = 0; \\ &-\frac{\lambda}{2} \int_{-t}^t \tau_{k-1}(x) F(t, x) dx + \tau_k(t) + \lambda \int_{-t}^t \tau_k(x) F(t, x) dx - \frac{\lambda}{2} \int_{-t}^t \tau_{k+1}(x) F(t, x) dx = 0; \\ &-\frac{\lambda}{2} \int_{-t}^t \tau_{n-1}(x) F(t, x) dx + \tau_n(t) + \lambda \int_{-t}^t \tau_n(x) F(t, x) dx = 0. \end{aligned} \right. \quad (7)$$

The resulting system contains  $n + 2$  unknown functions with  $n + 1$  equations, i.e. it is incomplete.

This system should be supplemented with equilibrium conditions. For each of the layers, the following equality is true:

$$\begin{aligned} \frac{dT_k}{dx} &= \tau_{k-1}(x) - \tau_k(x); \\ P_{k-1}(x) - P_k(x) &= \frac{T_k}{R_n}, \end{aligned} \quad (10)$$

where  $K=1, 2, 3, \dots, n+1$  and for  $T$ :

$$\begin{aligned} \sum T_k(-t) &= T_I, \quad \sum T_k(t) = T_{II}; \\ \int_{\alpha}^{t_0} \tau_0(x) - P_k(x) &= T_I - T_{II}, \end{aligned} \quad (11)$$

where  $T_I - T_{II} = \Delta T$  - circumferential preset force.

System (9) together with equilibrium equation (10), (11) should be supplemented with coulomb friction conditions

$$\tau_0(t) = fP_0(t), \quad \alpha < t < t_0 \quad (12)$$

**Solution of integral equation system**

The system of equations for determining becomes bulky enough, so we take the iterative method of solving.

At the first stage, we believe that with a given coefficient of friction and tension of the branches TI and TII, the law of distribution of tangent stresses within is given by the Euler formula. In this case, you can discard the first equation of the system (9) and in the second equation, the integral containing is transferred to the right. After solving the system and finding by formulae (10) we find. By and we find taking into account a clean bend, and, therefore, in a new approximation. With a large difference between and, the newly found should be considered as a new right-hand part of the system, and so on.

It is interesting to note that in such an iterative approach, the resolving system of equations has the same form as for the case of "pure" bending. This makes it possible, if necessary, to immediately take into account both bending stresses and stresses from the transmission of circumferential force. To do this, add functions (6) to the right side of the equation.

In the software solution of the problem, the iterative process simplifies the task if you use the reverse matrix of the foreground system.

To solve the system of integral equations, we will derive some auxiliary formulas. Due to the fact that the core of the integral equation linearly on the sections  $x < t$  or  $x > t$  relative to "X" has the form

$$F(t, x) = \begin{cases} (t-t)(t+x), & \text{in } x < t \\ (t+t)(t-x), & \text{in } x > t \end{cases} \quad (13)$$

output formulas for certain integrals.

designate 
$$\int \tau(x)dx = \tau^*(x)$$

$$\int \tau^*(x)dx = \iint \tau(x)dx = \tau^{**}(x)$$

Then we get at t outside the segment  $\alpha, \beta$ :

$$\int_{\alpha}^{\beta} \tau(x)F(t, x)dx = (t - zt) [(t + z\beta)\tau^*(\beta) - (t + z\alpha)\tau^*(\alpha) - z(\tau^{**}(\beta) - \tau^{**}(\alpha))],$$

где 
$$z = \text{Sign}(t - x) = \begin{cases} \text{lin} & t \succ x \\ -\text{lin} & t \prec x \end{cases}$$

и

$$\int_{\alpha}^{\beta} \tau(x)F(t, x)dx = (t - t) [(t + t)\tau^*(t) - (t + \alpha)\tau^*(\alpha) - \tau^{**}(t) + \tau^{**}(\alpha)] -$$

$$-(t + t) [(t - t)\tau^*(t) - (t - \beta)\tau^*(\beta) - \tau^{**}(t) - \tau^{**}(\beta)]$$

Let's replace coordinates by formula

$$x = U - \alpha \cos \theta, \quad dx = \alpha \sin \theta d\theta \tag{*}$$

где

$$U = \frac{\beta + \alpha}{2}, \quad \alpha = \frac{\beta - \alpha}{2}.$$

In  $x = \alpha, \theta = 0$  and in  $x = \beta, \theta = \pi$ .

We substitute the function sought on the segment  $\alpha, \beta$  in the form of a trigonometric interpolation Lagrange polynomial with interpolation nodes at the Chebyshev points:

$$\tau(x) = \sum_{j=1}^n \tau_j \frac{1}{n} \left[ 1 + 2 \sum \cos m\theta_j \cos m\theta \right] \tag{14}$$

where  $t_j$  is the polynomial coefficient;  $n$  is the number of interpolation points on the segment  $\alpha, \beta$  [theta]  $j =$  - interpolation nodes

The representation (14) makes it possible to calculate the functions  $\tau^*(x)$  and  $\tau^{**}(x)$ :

$$\tau^*(x) = \sum_{j=1}^n \tau_j \alpha \varphi_j^*(\theta) \quad \text{и}$$

$$\tau^{**}(x) = \sum_{j=1}^n \tau_j \alpha^2 \varphi_j^{**}(\theta).$$

where 
$$\varphi_j(\theta) = \frac{1}{n} \left[ -\cos \theta - \frac{\cos \theta_j \cos 2\theta}{2} + \sum_{m=2}^{n-1} \cos m\theta_j \left( \frac{\cos(m-1)\theta}{m-1} - \frac{\cos(m+1)\theta}{m+1} \right) \right],$$

$$\varphi_j^{**}(\theta) = \frac{1}{n} \left[ -\frac{\cos 2\theta}{4} + \frac{\cos \theta_j}{4} \left( \cos \theta - \frac{\cos 3\theta}{3} \right) + \cos 2\theta_j \left( \frac{\cos 2\theta}{3} - \frac{\cos 4\theta}{24} \right) - \right.$$

$$\left. - \frac{1}{n} \sum_{m=3}^{n-1} \cos m\theta_j \left( \frac{\cos(m-2)\theta}{(m-1)(m-2)} - \frac{\cos m\theta}{m^2 - 1} + \frac{\cos(m+2)\theta}{(m+1)(m+2)} \right) \right] \tag{15}$$

In here

$$\tau^*(\alpha) = \sum_{j=1}^n \tau_j \alpha \varphi_j^*(\theta), \quad \tau^*(\beta) = \sum_{j=1}^n \tau_j \alpha \varphi_j^*(\pi),$$

$$\tau^*(t) = \sum_{j=1}^n \tau_j \alpha \varphi_j^*(\theta_t)$$

Where

$$\tau^*(x) = \sum_{j=1}^n \tau_j \alpha \varphi_j^*(\theta) \quad \text{i}$$

$$\tau^{**}(x) = \sum_{j=1}^n \tau_j \alpha^2 \varphi_j^*(\theta).$$

$$\begin{aligned} \text{где } \varphi_j(\theta) &= \frac{1}{n} \left[ -\cos \theta - \frac{\cos \theta_j \cos 2\theta}{2} + \sum_{m=2}^{n-1} \cos m\theta_j \left( \frac{\cos(m-1)\theta}{m-1} - \frac{\cos(m+1)\theta}{m+1} \right) \right], \\ \varphi_j^{**}(\theta) &= \frac{1}{n} \left[ -\frac{\cos 2\theta}{4} + \frac{\cos \theta_j}{4} \left( \cos \theta - \frac{\cos 3\theta}{3} \right) + \cos 2\theta_j \left( \frac{\cos 2\theta}{3} - \frac{\cos 4\theta}{24} \right) - \right. \\ &\quad \left. - \frac{1}{n} \sum_{m=3}^{n-1} \cos m\theta_j \left( \frac{\cos(m-2)\theta}{(m-1)(m-2)} - \frac{\cos m\theta}{m^2-1} + \frac{\cos(m+2)\theta}{(m+1)(m+2)} \right) \right] \end{aligned} \quad (15)$$

При этом

$$\begin{aligned} \tau^*(\alpha) &= \sum_{j=1}^n \tau_j \alpha \varphi_j^*(\theta), \quad \tau^*(\beta) = \sum_{j=1}^n \tau_j \alpha \varphi_j^*(\pi), \\ \tau^*(t) &= \sum_{j=1}^n \tau_j \alpha \varphi_j^*(\theta_j) \end{aligned} \quad (16)$$

где

The same limit ratios are right also for  $\tau^{**}(x)$ .

The formulas introduced above allow you to apply the number of locations method to an integration line divided into a number of sections, on each of which the desired function has a smooth structure. In this task, the boundaries of the parcels will be the points of change of the external influences acting on it:

$$\begin{aligned} -l, -l_0 & \text{ - 1 - й участок;} \\ -l_0, \alpha & \text{ - 2 - й участок;} \\ \alpha, l_0 & \text{ - 3 - й участок;} \\ l_0, l & \text{ - 4 - й участок.} \end{aligned}$$

Note that interpolation points thicken to parcel boundaries.

So, we break the integration line  $2l$  into  $m$  sections, on each of which we take the decomposition (14) at  $nq$ ,  $q = 1, 2, 3, \dots, m$  interpolation points. Then the coefficients of the interpolation formulas will have an indexation, where  $q = 1, 2, 3, \dots, m$  is the number of the section on the integration line;  $m$  is the number of splitting sections of the integration line;  $k$  is the interlayer number in the multilayer tape;  $k = 1, 2, 3, \dots, n, n+1$  - number of layers in the tape;  $j$  is the number of interpolation points in the  $q$ th section.

To apply the above approach to solving the system of integral equations, we rewrite it in the form:

$$\begin{cases} \tau_1(t) + \lambda \int_{-l}^l \tau_1(x) F(t, x) dx - \frac{\lambda}{2} \int_{-l}^l \tau_2(x) F(t, x) dx = \frac{\lambda}{2} \int_{\alpha}^{l_0} \tau_0(x) F(t, x) dx + f(t) \frac{G}{h}; \\ -\frac{\lambda}{2} \int_{-l}^l \tau_1(x) F(t, x) dx + \tau_2(t) + \lambda \int_{-l}^l \tau_2(x) F(t, x) dx - \frac{\lambda}{2} \int_{-l}^l \tau_3(x) F(t, x) dx = f(t) \frac{G}{h}; \\ -\frac{\lambda}{2} \int_{-l}^l \tau_{k-1}(x) F(t, x) dx + \tau_k(t) + \lambda \int_{-l}^l \tau_k(x) F(t, x) dx - \frac{\lambda}{2} \int_{-l}^l \tau_{k+1}(x) F(t, x) dx = f(t) \frac{G}{h}; \\ -\frac{\lambda}{2} \int_{-l}^l \tau_{n-1}(x) F(t, x) dx + \tau_n(t) + \lambda \int_{-l}^l \tau_n(x) F(t, x) dx = f(t) \frac{G}{h}. \end{cases}$$

where  $f(t)$  is defined from formula (6), and  $\frac{1}{4}0$  in the first approximation by the formula obtained from (12):

$$\tau_0 = f \frac{T_0 - \frac{\Delta T}{2}}{R} e^{\frac{f}{R}(t_0 - t)}$$

Let us substitute the formula (18) into the system and attach the values by the same interpolation points, we obtain a system of equations of order. Let's take end-to-end numbering with unknown  $x_j$  for its description. The system of linear equations has the form

$$\sum_{j=1}^N \delta_{ij} x_j = b_i, \quad i=1, 2, 3, \dots, N \tag{20}$$

where

$$X_j = \begin{cases} \tau_j^{1,1} & \text{in } j \leq n_1 \\ \tau_{j-n_1}^{2,1} & \text{in } n_1 < j \leq n_1 + n_2 \\ \tau_{j-(k-1)\sum_{q=1}^m n_q}^{q,k} & \text{in } (k-1)\sum_{q=1}^m n_q + n_1 + n_2 + \dots + n_{q-1} < j \leq (k-1)\sum_{q=1}^m n_q + n_1 + n_2 + \dots + n_{q-1} + n_q \end{cases} \tag{21}$$

Taking into account the structure of the system (20) and the accepted indexation, to find  $\delta_{ij}$  we take the following computational procedure: Представим  $i$  и  $j$  в виде

$$\begin{aligned} i &= (k-1)\sum_{q=1}^m n_q + \sum_{q=1}^{k_1} n_q + i^1 \\ j &= (k-1)\sum_{q=1}^m n_q + \sum_{q=1}^{k_1} n_q + j^1 \end{aligned} \tag{22}$$

$$\begin{aligned} \text{then in } k = k^1 & \quad \delta_{ij} = \lambda F_1 + \delta_i^j \\ \text{in } |k = k^1| = 1 & \quad \delta_{ij} = -\frac{\lambda}{2} F_1 \\ \text{in } |k = k^1| > 1 & \quad \delta_{ij} = 0 \end{aligned}$$

where  $\delta_i^j = \begin{cases} 0 & \text{in } i \neq j \\ 1 & \text{in } i = j \end{cases}$  - symbol Kronoker.

To calculate  $F_1$ , the representation (22) gives:

- $k_1 + 1$  - number of integration area;
  - $j_1$  is the number of the interpolation coefficient of the polynomial;
  - $k_1 + 1$  - unit force application area number;
  - $i^1$  is the point number of unit force application on the site.
- Formula (\*) taking into account (22) shall be recorded as  $t_i = U_{k_1+1} - \alpha_{k_1+1} \cos \theta_i$  (23)

Enter the same conditional distance to the  $x_j$  point:

To calculate  $F_1$ , the representation (22) gives:

- $k_1 + 1$  - number of integration area;
  - $j_1$  is the number of the interpolation coefficient of the polynomial;
  - $k_1 + 1$  - unit force application area number;
  - $i^1$  is the point number of unit force application on the site.
- Formula (\*) taking into account (22) shall be recorded as  $t_i = U_{k_1+1} - \alpha_{k_1+1} \cos \theta_i$  (23)

Enter the same conditional distance to the  $x_j$  point:

Enter the same conditional distance to the  $x_j$  point:

$$X_j = U_{k_1+1} - \alpha_{k_1+1} \cos \theta_i \tag{24}$$

Then we get it at  $k^1 \neq k^2$ :

$$F_1 = F_1^* = \alpha_{k^1} (t - zt_{i^1}) \begin{bmatrix} (t + z\beta_{k^1+1})\varphi_{1j^i}^{k^1+1}(\pi) - (t + z\alpha_{k^1+1})\varphi_{1j^i}^{k^1+1}(0) - \\ -z\alpha_{k^1+1}(\varphi_{2j^i}^{k^1+1}(\pi) - \varphi_{2j^i}^{k^1+1}(0)) \end{bmatrix}, \quad (25)$$

where  $z = \text{Sign}(t-x_j)$ .  
in  $k^1 = k^1$

$$F_1 = \alpha_{k^1} (t - t_{i^1}) \left[ (t + t_{i^1})\varphi_{1j^i}^{k^1+1}(\theta_{i^1}) - (t + \alpha_{k^1+1})\varphi_{1j^i}^{k^1+1}(0) - \alpha_{k^1+1}(\varphi_{2j^i}^{k^1+1}(\theta_{i^1}) - \varphi_{2j^i}^{k^1+1}(0)) \right] - \\ - (t + t_{i^1})\alpha_{k^1} \left[ (t - t_{i^1})\varphi_{1j^i}^{k^1+1}(\theta_{i^1}) - (t + \beta_{k^1+1})\varphi_{1j^i}^{k^1+1}(\pi) - \alpha_{k^1+1}(\varphi_{2j^i}^{k^1+1}(\theta_{i^1}) - \varphi_{2j^i}^{k^1+1}(\pi)) \right] \quad (26)$$

The above formulas allow you to find the coefficient of interpolation polynomials, and therefore the values of tangent stresses. You can also see that the task is easily programmed.

Knowing the tangent stresses  $\tau_k(x)$  and the tensile forces in each layer, we find by the formula  $T_k$ :

$$T_k = \frac{T_0 - \frac{\Delta T}{2}}{n+1} + \int_0^x [\tau_{k-1}(x) - \tau_k(x)] dx \quad (27)$$

which, with the accepted interpolation formulas for the integration section  $q^1$ , will take the form

$$T_k = \frac{T_1}{n+1} + \sum_{q=1}^{q^1-1} \sum_{j=1}^{n_q} \tau_j^{q^1k} F_1^* + \sum_{j=1}^{j^i} \tau_j^{q^1} \alpha_q^1 (t - t_{i^1}) \begin{bmatrix} (t - t_{i^1})\varphi_{1j^i}^{q^1}(\theta_{i^1}) - (t + \alpha_{q^1})\varphi_{1j^i}^{q^1}(0) - \\ -\alpha_{q^1}(\varphi_{2j^i}^{q^1}(\theta_{i^1}) - \varphi_{2j^i}^{q^1}(0)) \end{bmatrix} \quad (28)$$

After that, for the region  $-l_0, +l_0$  it is possible to construct a recursive formula for sequentially finding the compression force of the fiber:

From the above iteration process, it is clear that the deformation of the compression of the layers across the fibers can be taken into account according to the premise (3).

$$P_{k-1}(x) = \frac{T_k}{R_n} + P_k(x)$$

### Results solution of system of integral equations

The solution of the system of integral equations gave the patterns of change in stresses in the belt during tension, bending and circumferential force.

On Fig. 4. shows a graph of the variation of shear stresses from the circumference of the girth arc in the five gasket conveyor belts, from which it follows that maximum stresses occur in layers located closer to the drum surface in the zone of the boundary of the transition from the resting angle to the sliding angle.

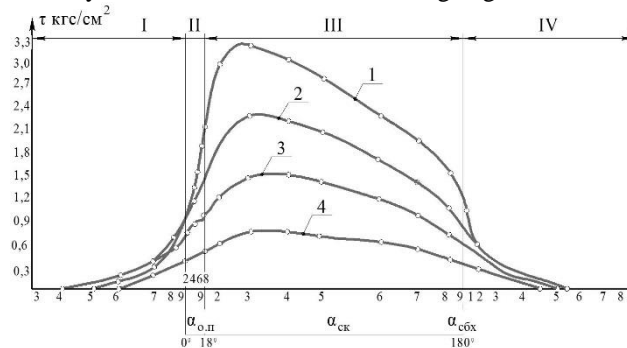


Fig. 4. Plot of change in shear stresses from circumferential girth arc force in five PAS- 250/120 shim conveyor belts.



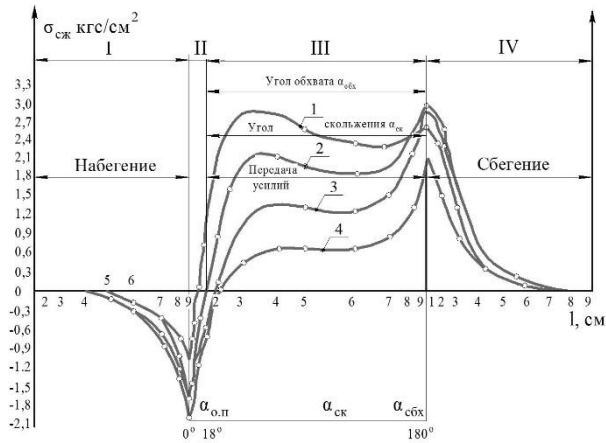


Fig. 5. Plot of change of shear stresses in rubber interlayers along the girth arc with joint action of stretching, bending and circumferential force in five PAS - 250/120 shim conveyor belt

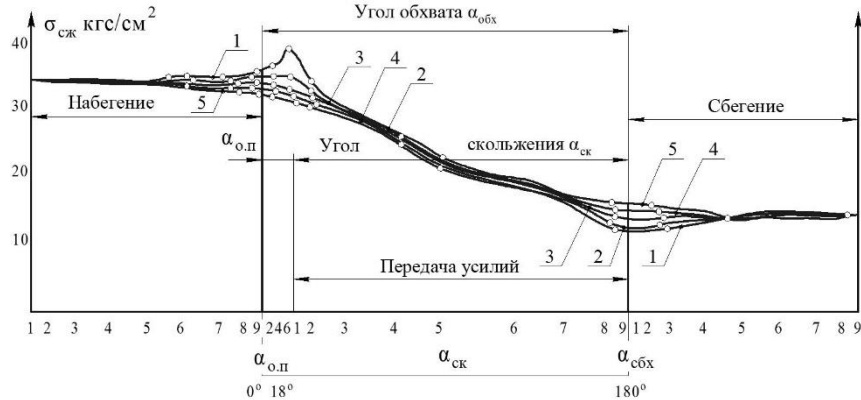


Fig. 6. Plot of change of tensile stresses along the girth arc in five gasket conveyor belt under action of circumferential force and tension

Graphs of changes in total shear stress values along the length of the girth arc under the combined action of tension, bending and circumferential force (Figure 5) show that the circumferential force has a significant effect on the amount and nature of the distribution of shear stress between the tape layers.

A graph of tensile stresses in the tape gaskets along the length of the girth arc under the action of tension and circumferential force (Figure 6) shows that maximum tensile stresses occur in the gaskets located closer to the drum surface in the area of the boundary of the relative rest angle and sliding angle. As the tensile stresses decrease from the point where the belt runs onto the drum on the girth arc, the tensile stresses decrease and the minimum value is at the point where they run off the drum surface.

The pattern of the distribution of tensile stresses between the belt gaskets under the combined action of stretching, bending and circumferential force is shown in Fig. It follows from the graph that the tensile stresses between the gaskets can be unevenly distributed.

Gaskets located closer to the drum surface are less loaded. Maximum tensile stresses occur in the outer gaskets near the boundary of the relative rest angle and sliding angle. From the graphs on Fig.7. it should be understood that by varying the ratios of tensile forces, circumferential forces and drum diameters, it is possible to achieve the equality of tensile stresses in all gaskets.

With the combined action of stretching, bending and circumferential force, compressive stresses arise in rubber layers, caused by the action of overlying stretched gaskets on the underlying ones.

A graph of the change in compressive stresses between the gaskets of the five gasket conveyor belts is shown in Fig. 8. It can be seen from the graph that stresses in gaskets in the area of relative rest angle are constant and gradually decrease in the area of sliding angle. The maximum values of compression stresses are acquired in the lower layers.

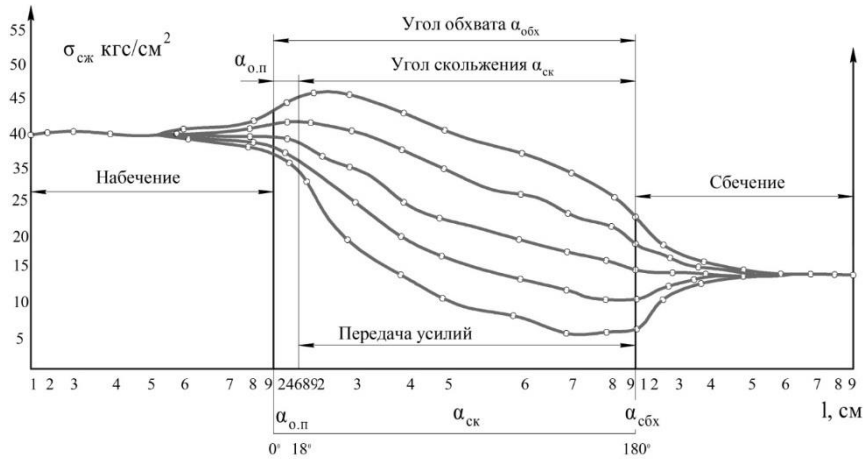


Fig. 7. Plot of tensile stress changes in the gaskets along the girth arc under the combined action of tensile, bending and circumferential force in the PAS - 250/120 five-layered conveyor belt

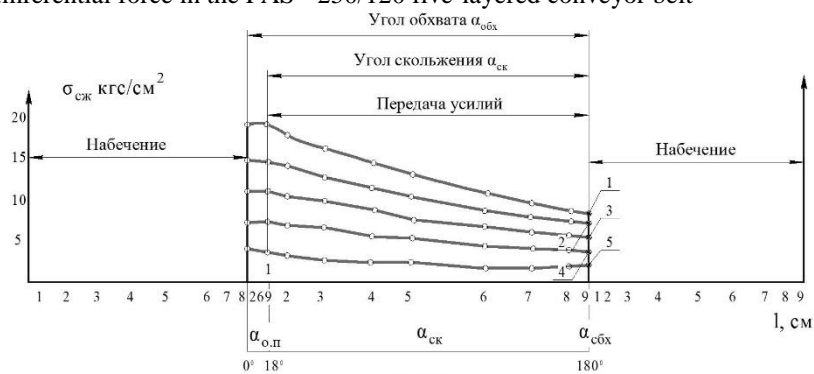


Fig. 8. Plot of change of total compressive stresses between gaskets along the length of girth angle in PAS - 250/120 five-layered conveyor belt

On Fig. 9. graph of compression stress versus drum diameter is shown. As drum diameter increases, compression stresses in gaskets decrease.

On Fig. 10. shows a graph of the dependence of compression stresses on belt tension, from which it follows that as the tension increases, the compression stresses increase. It should be noted that as the tension of the belt increases to 100 kgf per centimeter of the width of the belt, the values of compression stresses in 1, 2, and 3 layers from the surface of the drum increase according to a linear law, and when the tension increases to 140 kgf per centimeter of the width of the belt, an increase in the speed of their increase is observed. The rate of stress increase in the 4 and 5 layers remains constant.

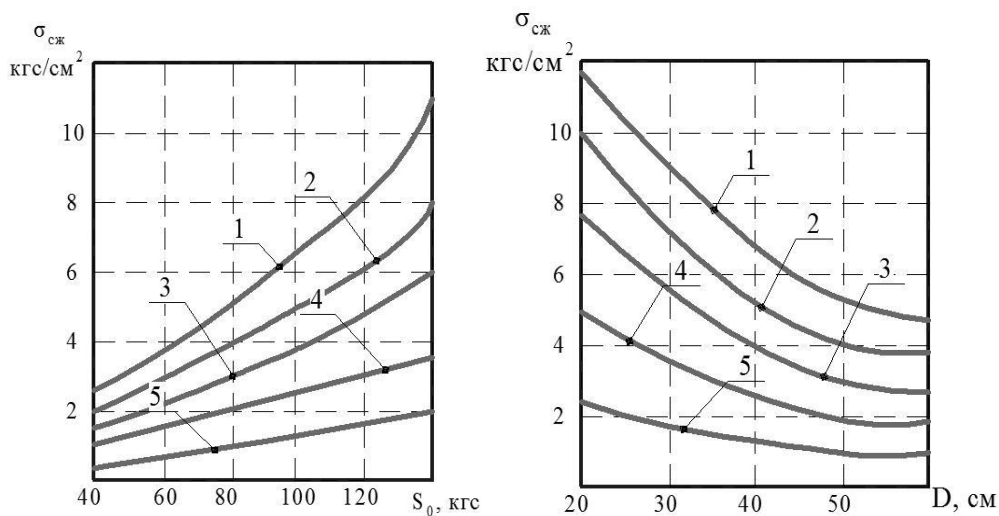


Fig. 9. Dependence of compressive stresses on diameters of drums in five gasket conveyor PAS Tape - 250/120

Fig. 10. Compressive Stress Dependence on Tensile Forces in Five PAS - 250/120

The compression stresses combined with the shear stress cause gradual fatigue failure of the interlayers under belt operating conditions, especially at small drum diameters and high belt tension.

As the studies [2] show, fatigue destruction of the belt from periodic bends on the drums and support rollers occurs, as a rule, by delamination of its frame.

To assess the durability of the tape in this case, a calculation based on the law of summation of damages [2.8] is used.

Based on the experiments, it has been found that the number of cycles  $N$  before the destruction of the tape and the stresses at which the destruction occurs are related  $\sigma \sum$  a dependence that is also true for other materials. Therefore, when determining the service life of tapes from fatigue conditions on drums and on support rollers, the design dependencies proposed by D.N. Reshetov [9] for the condition of summation of damages are taken as the initial ones:

$$\begin{aligned} \sum \sigma_i^{m_1} N_{1i} &= \text{const}, \\ \sum \tau_i^{m_2} N_{2i} &= \text{const}, \end{aligned} \quad (30)$$

where  $\sum$  is the sign of summation by the number of different values of variable stresses;  $\sigma_i$ ,  $\tau_i$  is one of the values of variable stresses;  $m_1$ ,  $m_2$  - measure of degree of equations of fatigue curves;  $N_{1i}$ ,  $N_{2i}$  - the total number of load cycles at stresses  $\sigma_i$ ,  $\tau_i$ .

The service life of the belt in hours  $T_g$  when moving on one drive drum and in constant operation can be determined as follows:

where  $N_1$  is the number of cycles before destruction;  $t_1$  is the time the belt traverses the conveyor loop (one cycle time).

Time of one cycle  $t_1$  in hours

$$t_1 = \frac{L_n}{3600V_n} \quad (32)$$

где  $L_n$  – длина конвейерной ленты;  $V_n$  – скорость движения конвейерной ленты.

Число циклов до разрушения определится из уравнения кривой усталости:

$$N_1 = \frac{C}{\sigma_{1\max}^{m_1}} \quad (33)$$

Based on dependencies (32), (33), (34), we obtain:

$$T_c = \frac{L_n C_1}{3600 V_n \sigma_{1\max}^{m_1}} \quad (34)$$

When moving along the conveyor contour, the belt bends on drums of different diameters and with different initial tensile forces, i.e. the maximum variable stresses during tension and bending at different points of the conveyor have different values. The maximum variable voltages with respect to which durability is calculated are also affected by the variability of the conveyor operation mode (start, stop, work under load, work without load). Studies by N.Y. Bilichenko et al. [8] show that significant dynamic loads can occur in the belt during the start-up and stop of the conveyor. Greater acceleration of the belt during start-up may occur due to poor tensioner performance as well as low initial belt tension. Therefore, it is necessary to take into account the effect of the difference in drum diameters, tape tension variability and operating mode in the durability calculations.

These factors can be taken into account by the respective factors [2.9] and presented as a dependency:

$$T_1 = T_0 \frac{1}{n_1} K_i K_{1\text{неп}} \quad (35)$$

where  $k_{1\text{неп}}$  is the operating mode variability factor;  $k_i$  is a coefficient that takes into account the variability of drum diameters (can be determined from the equation proposed by D. N. Reshetov for calculating belt gears);  $T_1$  - tape durability when moving on drums;  $n_1$  is the number of reels.

The variable coefficient of operation mode can be determined by analogy based on the procedure given in works [2.9]

$$K_{1\text{неп}} = \sqrt[m_1]{\sum \left( \frac{\sigma_i}{\sigma_1} \right)^{m_1} \frac{t_i}{t}} \quad (36)$$

where  $\sigma_i$  - tensile stresses and tape bending on the drum under mode  $i$ ;  $\sigma_1$  is the voltage with respect to which the variable coefficient of the operating mode is calculated;  $t_i$  - operating time in mode  $i$ ;  $t$  is the total design operating time.

Traction force variability factor:

$$K_{p_0} = \frac{N}{N_i} \quad (37)$$

The coefficient of variability of drum diameters can be determined from the equation proposed by D. N. Reshetov for calculating belt gears [9].

$$\sigma_{1\max}^{m_i} \frac{N}{K_i} = (\sigma_{1\max}^{m_i} + \sigma_{2\max}^{m_i} + \dots + \sigma_{n\max}^{m_i}) \frac{N}{n_i} \quad (38)$$

from this it follows that

$$K_i = \frac{\sigma_{1\max}^{m_i} n_i}{\sum_{i=1}^n \sigma_{i\max}^{m_i}} \quad (39)$$

where N is the number of cycles until destruction without traction force; Ni is the number of cycles before failure in mode i.

#### Experimental studies

To verify the analytical description, a laboratory study of fatigue wear of ribbons during stretching, bending on drums and transmission of traction force was designed and manufactured, the experimental installation resting on Fig.11,12

The installation consists of two pulleys 1 on which the sample tape 2 is put. Upper pulley is fitted on shaft of electric motor 3, lower pulley is placed in holder 4, to which force is applied through dynamometer 5 by means of lever system 6, load 7 and load screw 8, which stretches sample [10].

Lower pulley is connected by means of cardan shaft 9 to alternator 10 feeding lamp rheostat 12, which serves as load on drum shafts. The torque is changed by means of a lamp rheostat.

Samples of 50 mm wide tape were tested, in which cutouts were made to avoid friction against the sides of the pulley. Observations were carried out on sections of the tape 100 mm long. Tape samples were joined prior to installation on pulleys by vulcanization. The number of revolutions of the pulleys was fixed by electric speed counters P connected to the pulley shafts.

The experiments were carried out in such a sequence.

An initial tension was reported to a belt sample dressed on pulleys and an electric motor was turned on. To prevent overheating of the tape and its inspection, the installation stopped periodically. The sample was tested until complete stratification [11].

To determine the number of loading cycles before tape delamination, the ratio K of the sample length to the length of the pulley girth arc was first found;

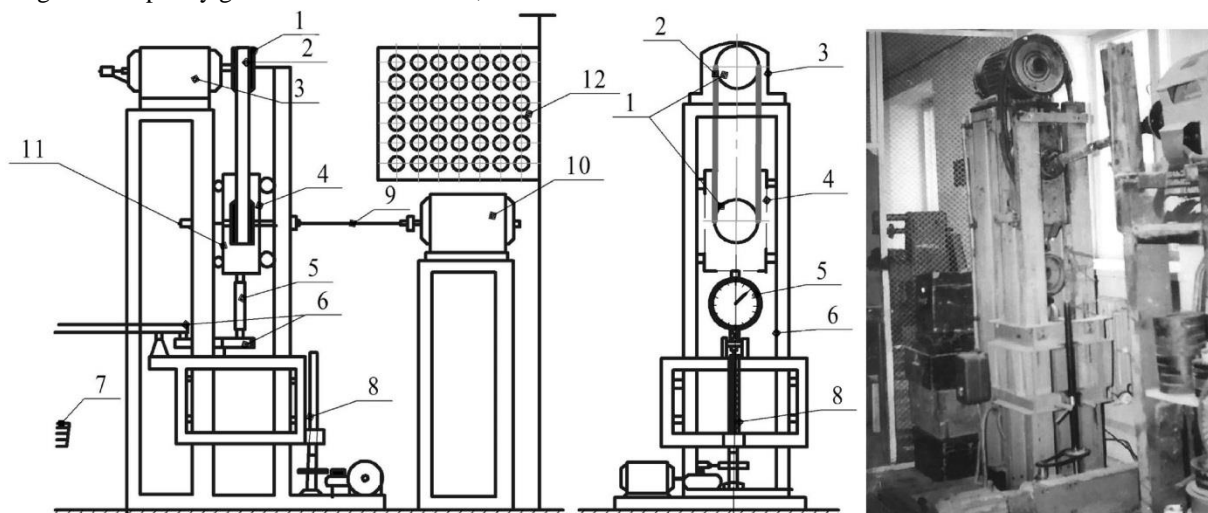


Рис.11. Схема установки

Рис.12. Общий вид установки

$$K = \frac{l_o}{l_{uu}} = \frac{\pi R + A}{\pi R},$$

where  $l_o$  is the length of the sample;  $l_{uu}$  is the length of the girth arc; A is the center-to-center distance; R - pulley radius;  $n_1$  - average number of pulleys revolutions before sample destruction.

$$n^1 = \frac{n_1 + n_2}{2},$$

where  $n_1$  and  $n_2$  are readings of drum rpm counters.

The center-to-center distance  $A$  was measured at the beginning and end of the experiment, after which the average value was calculated.

The length of the test belt samples was significantly shorter than the length of the conveyor belt. Therefore, it was possible to assume the effect on the results of the large-scale factor trials. With a slight distortion of the linear scale in the model, phenomena of the same kind arise as in nature [12] A.T. Nazarov believes that the manifestation of a large-scale effect should be expected in cases where the static similarity of the materials of the model and nature is violated, that is, the number of defects in the model and nature is in different ratios.

The influence of the scale factor in the tests of conveyor belts has not yet been sufficiently studied, although the sizes of the width of the samples recommended by GOST 20-62 - 25.0 and 50.0 mm to some extent take into account this influence. For example, the non-simultaneous coefficient of tearing of gaskets, according to the recommendations of the standard, is 0.74. The coefficient of loss of strength of the tape sample due to violation of the integrity of the extreme warp threads when cutting samples from the tape is taken into account according to the recommendations of the standard by reducing the load by 5%.

The use of smaller width samples can lead to errors in determining the mechanical characteristics of tapes. To avoid them, only standard 25.0 mm and 50.0 mm wide samples were used in the study.

To determine the fatigue limit of the tape, you must break the samples at several stress values. With an atom, there can be two variants of the study:

- the tape is tested at constant tension, but the diameters of the drums vary;
- the diameter of the drums is constant, but the tension of the belt changes.

As the test experiments showed, the tests on both of these methods give close results. Based on the analysis, it was found that in the conditions of stretching, compression and transmission of traction in the belts, tangent stresses are of significant importance.

According to the author, it is these stresses that cause fatigue destruction of the tape layers.

Therefore, in assessing the fatigue strength of the belts, it was decided to take into account the tangent stresses in the rubber layers and consider them together with the tension stresses in the fabric pads.

At each given amplitude  $S$  of voltage changes per cycle, upon reaching a certain number of  $N$  cycles, tape stratification occurs. The number of loading cycles before the belt delamination increases with a decrease in amplitude  $S$ . The results of an experimental study of the dependence of  $S$  on the  $N$  butt to the conclusion that the largest value of periodically changing stress exists, which the conveyor belt can withstand almost indefinitely. We can assume the existence of some limit of endurance.

Fatigue strips formed as a result of multiple cyclic loading gradually turn into a crack.

It is natural to assume that the number of loading cycles  $N$ , which causes the sample to break, is a decreasing function of the crack size and its minimum corresponds to the largest crack in its dimensions [2].

The number of cycles  $N$  before tape resolution must be subject to a specific distribution law. In the study presented, it is accepted that this distribution is most correctly subject to the law:

$$P_{III}, I(x) \tag{15}$$

In the analysis of the results of fatigue tests, it is convenient to consider the additional probability of  $I$  - i.e. the probability of non-failure of the sample at  $X = N$  cycles, which can be expressed as follows:

$$L_s(N) = \begin{cases} e_j^{-z^\alpha} & \text{in } N > N_{os} \quad j \leq n_1 \\ 1 & \text{in } N \leq N_{os} \leq n_1 + n_2 \end{cases} \quad z = \frac{N - N_0(\sigma_{изг} + \sigma_{P_0})}{V(\sigma_{изг} + \sigma_{P_0})N_0(\sigma_{изг} + \sigma_{P_0})} \tag{40}$$

n-failure equal to

To simplify the analysis without a large error, one can accept, which makes it possible to go to the law, that is, to a double indicative law, where

The probability of non-failure will now take the form: where  $L_s$  is the probability of non-failure of the sample for  $x = N$  cycles at the magnitude of change in voltages  $S$ ;  $N_{os}$  is the largest number of cycles, which at this total voltage  $S$  does not cause destruction;  $V_s$  or number of cycles  $N$  corresponding to probability of no

$$L_s(N) = e^{-e^y}$$

where

$$y = \alpha(\ln N - \ln V_s)$$

To estimate the probability parameters and to display the results of fatigue tests on the graphs, the number of cycles  $N$  before splitting the tape samples will be arranged in a variation series:

$$N_1 < N_2 < N_3 < \dots < N_n \tag{41}$$

where:  $n$  is the number of samples tested. Then we calculate the sequence of logarithms

$$x_1 < x_2 < \dots < x_m < \dots < x_n, \tag{42}$$

where

$$x_m = \lg N_m \text{ и } m = 1, 2, 3, \dots, n$$

In accordance with the calculations, we determine the corresponding probabilities:

$$P_m = 1 - \frac{m}{n+1} \quad (43)$$

Having determined the values, we find by the formula:

$$y_m = 2,30261 \lg(-\lg P_m) + 0,83405 \quad (44)$$

Based on the calculation data, we plot the depositions along the horizontal axis on a natural scale, and along the vertical axis the values of  $y =$  on a natural scale or their corresponding probabilities ( $P$ ) on a functional scale., Lie near a line whose equation

$$y = \alpha_s (x - u_s) \quad (45)$$

or

$$x = u_s + \frac{y}{\alpha_s} \quad (46)$$

where

$$u_p = \lg V_p$$

To determine the parameters, we calculate the average arithmetic and the average quadratic deviation of the values

$$x_m = \lg N_m \quad (47)$$

$$\lg N_m = \frac{1}{N} \sum_{i=1}^n \lg N_i$$

and

$$S(\lg N_m) = \sqrt{\frac{1}{n-1} \sum_{i=1}^n (\lg N_i - \lg N_m)^2} \quad (48)$$

Then we find the parameter values from the relations

$$\frac{1}{\alpha_s} = \frac{S(\lg N_m)}{\sigma_n} \quad (49)$$

$$u_s = \lg N_m + y_m \frac{1}{\alpha_s} \quad (50)$$

where coefficients are taken from 10.5.2 of probability theory course [12].

Variation series of numbers of cycles before destruction, sequence of logarithms corresponding to these numbers, calculated by formula (3) of probability estimation and value values based on results of fatigue tests of tape samples at corresponding stresses are summarized in Table-1

Table-1

№	$N_m$	$x_m = \lg N_m$	$x_m^2$	$P_m$	$y_m$
1	69500	4,8419	23,4439	0,909	-2,3496
2	72500	4,8603	23,6225	0,818	-1,6050
3	74000	4,8692	23,7091	0,727	-1,1431
4	74500	4,8721	23,7373	0,636	-0,7928
5	74500	4,8721	23,7373	0,545	-0,4993
6	80000	4,9030	24,0394	0,454	-0,2361
7	81000	4,9084	24,0923	0,363	0,0132
8	82500	4,9164	24,1709	0,273	0,2710

9	83500	4,9216	24,2221	0,181	0,5360
10	85500	4,9319	24,3236	0,090	0,8788
		48,8969	239,0984		

According to the table value

$$\lg N_m = \frac{48,8969}{10} = 4,88969$$

$$S(\lg N_m) = \frac{239,0984 - \frac{(48,8969)^2}{10}}{10} = 0,0276$$

Then we find the parameter values from the relations

$$\frac{1}{\alpha_s} = \frac{S(\lg N_m)}{\sigma_n} = \frac{0,0276}{1,0} = 0,0276 \quad \alpha_s = 36,23$$

$$u_s = \lg N_m + y_m \frac{1}{\alpha_s} = 3,8897 + 0,5117 \cdot 0,0276 = 4,9038$$

where and taken as per Table 10.5.2 [12]. The equation of our line will be:

$$y = 36.23 / x - 4.9038 /$$

Having previously set the probability of non-breakdown of samples, from the graph you can determine the number of cycles before their stratification.

On the basis of the obtained data, the fatigue curves of the three types of ribbons are constructed with a probability of non-failure of 0.5 and 0.9 in coordinates and, (Fig. 13.14).

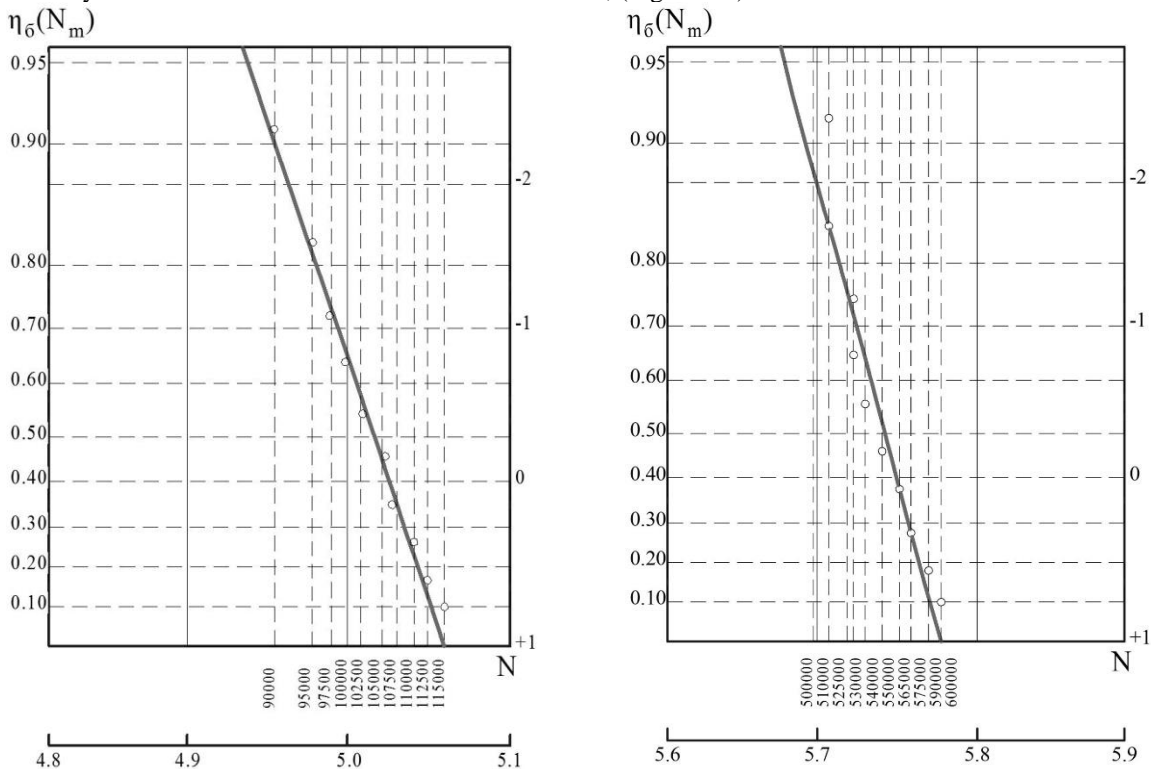


Fig. 13. Dependency Graph

- . (capron-based five-layered conveyor belt PAS-250/120 = 40 kgf/cm.p., = 5 kgf/cm.p.)

Fig. 14. Dependency Graph

- . (three-layered capron-based conveyor belt TK-300 = 50 kgfs / see the ave., = 8 kgfs / see the ave.)

It follows from the graphs that the fatigue curves of the tapes with a decrease in the current stress approach the same value for each type of tape - the fatigue limit.

It follows from the graphs drawn in logarithmic coordinates that the dependence on is satisfactorily approximated by the linear function

$$\lg(\sigma_{\text{пост}} + \sigma_{P_o} + \sigma_u) + m \lg N = C \quad (51)$$

By entering symbols  $\lg(\sigma_{\text{пост}} + \sigma_{P_o} + \sigma_u) = y$  и  $\lg N = x$ , we get the equation:

$$y = c - m x, \quad (52)$$

In which the constant factor  $m$  and  $c$  for a given material and loading conditions are unknown. Using the least squares method [12], we obtain the following expressions to determine these coefficients:

$$m = \frac{n \sum_{i=1}^n \lg(\sigma_{\text{пост}} + \sigma_{P_o} + \sigma_{\text{нст}})_i \lg N_i - \sum_{i=1}^n \lg N_i \sum_{i=1}^n \lg(\sigma_{\text{пост}} + \sigma_{P_o} + \sigma_u)_i}{n \sum_{i=1}^n (\lg N_i)^2 - (\sum_{i=1}^n \lg N_i)^2}$$

$$C = \frac{\sum_{i=1}^n \lg(\sigma_{\text{пост}} + \sigma_{P_o} + \sigma_u)_i}{n} - m \frac{\sum_{i=1}^n \lg N_i}{n} \quad (53)$$

Numerical values of coefficients  $m$  and  $c$  and values of fatigue limits for tested tape types under different loading modes are given in Table-2

Table-2

Values of fatigue curve coefficients and fatigue limits of tested tapes

Типы лент	Voltages on drums kgf/cm.p..	Fatigue limit kgf / see the ave.	m	C	m*	C*
Capron-based tape 250/120 five-layered, manufactured by the GDR.	30	35	0,227	2,51	4,4	10 <sup>11</sup>
	18,62	35	0,212	2,74	4,7	7,6·10 <sup>12</sup>
Capron-based tape TK-300 three-layered	34	40	0,094	2,04	10,62	1,8·10 <sup>23</sup>
Capron-based tape TK-300 eight-layered	12,75	38	0,384	4,12	2,6	5·10 <sup>10</sup>
	30	38	0,588	4,29	1,7	2,1·10 <sup>7</sup>

The stress and number of cycles can also be represented as a power constraint of the

$$(\sigma_{\text{пост}} + \sigma_{P_o} + \sigma_u)^{m^*} N = C^* \quad (54)$$

where is a constant value, and the index of degree  $m^*$  is equal to the cotangence of the slope angle of the fatigue dependence graph in logarithmic coordinates of the axis. The coefficients  $m^*$  and are related to the coefficients  $m$  and  $C$  as follows:

$$m^* = \frac{1}{m} \quad \text{и} \quad m^* C = \lg C^*$$

The values of the coefficients  $m^*$  and are given in the table above.

In the preceding studies [2.13], it has been shown that as a result of cyclic tensile loads, the fabric gaskets of the tape wear, and when bending on the drums, they are delaminated with the destruction of the rubber layers. It is believed that this failure is mainly caused by shear stresses resulting from uneven elongation of the fabric pads. The shear stress in the belt is also due to the transmission of traction force from the drive drum. The effect of the transmitted traction forces on the durability of multi-laying belts has not yet been investigated to the necessary extent, as indicated in the work of N.Ya. Bilichenko [8].

Changes in tensile stresses and deformations of gaskets [2] are also insufficiently investigated.

Tape samples were tested at constant tension and drum diameter. The circumferential force varied. The change in the circumferential force was carried out by changing the power consumed from the generator by the lamp rheostat.



The power consumed by the lamp rheostat varied in stages: 0; 2,5; 4.2 and 5 kW.

Two types of tapes were tested: TK-300 eight-lined, PAS-250/120 five-lined production of the GDR and TK - 300 three-lined.

Stresses in tape samples were determined on the basis of the following data: modulus of elasticity, respectively  $E_1 = 300 \text{ kgf/cm}^2$ ,  $E_2 = 2500 \text{ kgf/cm}^2$  and  $E_3 = 3000 \text{ kgf/cm}^2$ ; rubber shear modulus  $G_{1,2,3} = 15 \text{ kgf/cm}^2$ , distance from drum surface to upper gasket  $h_1 = 0.14 \text{ cm}$ ,  $h_2 = 1, 2 \text{ cm}$ , and  $h_3 = 1.6 \text{ cm}$ ; fabric gasket thickness  $= 0.14 \text{ cm}$ ,  $= 0.1 \text{ cm}$  and  $= 0.1 \text{ cm}$ ; thickness of rubber layer  $= 0.08 \text{ cm}$ ,  $= 0.06 \text{ cm}$  and  $= 0.04 \text{ cm}$ .

Based on processing of experimental data, graphs of dependence of number of cycles before stratification on value of circumferential force at probability of non-destruction 0.5 and 0.9 (Fig. 15) are constructed.

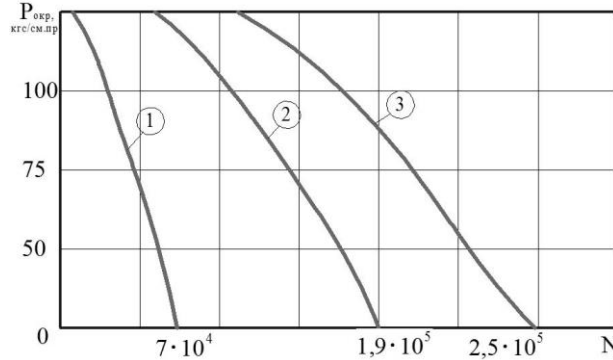


Fig. 15. Graph of cycle number versus district force. 1-PAS-250/120 five-layered,  $= 61,030 \text{ kgf/cm.pr}$ , 2, 3-TK-300/three-layered,  $= 71,780$  and  $49.00 \text{ kgf/cm.pr}$

It has been found that the force has a significant effect on the intensity of delamination. As the traction force increases, the number of cycles before the tape delamination decreases. Therefore, the tangential stresses generated in the rubber layers of the belt under the conditions of its interaction with the drive drum are increased. This is also evidenced by the results of observations on the nature of destruction of the tested samples.

At smaller circumferential force (0, 20, 50 kgf) delamination takes place between gaskets above neutral layer. However, as the circumferential force increases, it moves closer to the surface of the drums. Usually, the stratification of samples begins with the appearance of microcracks, which then spread along the length of the interlayer and merge, form a zone of continuous destruction.

The displacement of the breakable interlayers to the drum surface with an increase in traction force confirms the assumption with the occurrence of tangent stresses, which mainly cause the destruction of the rubber interlayers. The study shows that due to the occurrence of bending stresses and circumferential force, the compression stresses in the lower layers generally disappear and the gaskets work only for tension. There is an optimal number of gaskets, exceeding which does not lead to a decrease in stresses.

### Conclusions

Based on the analysis and mathematical description of the above dependencies, the following formula is proposed for determining stresses from bending:

$$\sigma_u = \frac{Eh\delta(i - 2k + 1)}{D} \left(\frac{3G}{E}\right)^{0,01}, \text{ kgf/cm.pr} \quad (55)$$

where is the modulus of elasticity of the layer,  $\text{kgf/cm}^2$ ;  $\delta$  - thickness of the fabric gasket with a rubber layer,  $\text{cm}$ ;  $i$  - thickness of the fabric gasket,  $\text{cm}$ ;  $k$  - number of gaskets in the belt;  $n$  - layer number,  $= 1, 2, 3, \dots, n$ ;  $G$  - rubber shear modulus,  $\text{kgf/cm}^2$ ;  $D$  - drum diameter,  $\text{cm}$ .

To determine the stress from the circumferential force, the formula is proposed:

$$\sigma_{P_o} = \frac{\Delta S}{2iB} \left(\frac{E}{3G}\right)^{0,02}, \text{ kgf/cm.pr} \quad (56)$$

where is the circumferential force,  $\text{kgf}$ ;  $B$  is the width of the tape,  $\text{cm}$ . Total stress from tension, bending and circumferential force is:

$$i_{gon} = \frac{\sigma_{gon} + \frac{EH\delta}{D} \left(\frac{3G}{E}\right)^{0,01} - \sqrt{\left[\sigma + \frac{EH\delta}{D} \left(\frac{3G}{E}\right)^{0,01}\right]^2}}{\frac{2EH\delta}{D} \left(\frac{3G}{E}\right)^{0,01}} - \frac{\frac{4EH\delta}{BD} \left(\frac{3G}{E}\right)^{0,01} \left[\frac{\Delta S}{2} \left(\frac{E}{3G}\right)^{0,02} + S_p\right]}{\frac{2EH\delta}{D} \left(\frac{3G}{E}\right)^{0,01}} \quad (58)$$

The formula is valid with a positive value for a subcortical expression.

The allowable stresses in the synthetic conveyor belt gaskets can be considered equal (0.2 - 0.35).

Thus, the proposed calculation technique allows determining the required number of gaskets in the belt at a given allowable stress and known tension, the width of the belt, as well as the diameter of the drum.

In Fig. 16. shows changes in stress in the belt depending on the number of gaskets. It follows from the graphs that the low stress region corresponds to the static safety margin interval for synthetic tapes from 7 to 9. Usually, the safety margin of the tapes is taken much higher. This leads to an unreasonable increase in the number of gaskets and therefore to an increase in the cost of the tape. According to the strength conditions of the gaskets, a six-layered tape can be used instead of an eight-layered tape. It will be appreciated, however, that under the conditions of conveying coarse materials, stresses arising from the fall of coarse pieces in the loading units may be a criterion for selecting the thickness of the belt.

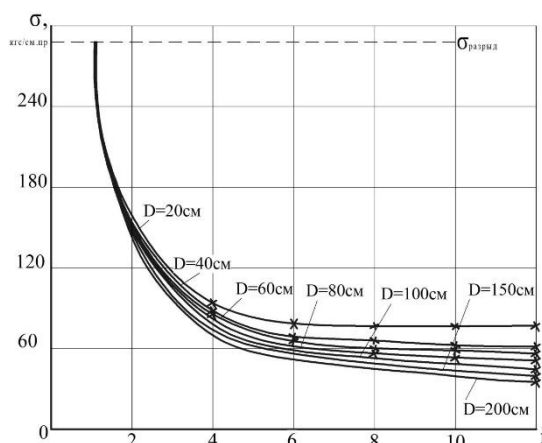


Fig. 16. Plot of stress in capron-based conveyor belt gaskets versus number of gaskets during tension, bending and circumferential force.

Method of calculation of conveyor belts for endurance is proposed, which allows to take into account fatigue phenomena arising during interaction of belt with driving and deflecting drums and support rollers [14].

Fatigue characteristics of belts at variable stresses caused by bending, stretching and transmission of traction force can serve as a criterion for selection of diameter of drive and deflecting drums and belt tension at all sections of conveyor. If the tape is used in a mode in which the variable stresses do not exceed the fatigue limit, the tape will not delaminate during the period of operation.

It is proposed to determine the preliminary tension of the tape under conditions of stretching, bending and circumference by the formula;

$$S_{\max} = \left[ \sigma_m K_{p_0} - (\sigma_{p_0} + \sigma_u) \right] \frac{Bi}{n_0} \quad (59)$$

where  $\sigma_m$ -limit of belt fatigue at tension, bending and circumferential force, kgf/cm.pr; - coefficient taking into account traction forces; - stresses from circumferential force, kgf/cm.pr; - stresses from bending, kgf/cm.pr; - number of gaskets; - reserve of strength in bending and circumferential force on drums, Stresses and are determined by formulas (55), (56).

The permissible tension of the belt under the joint action of loads from the bending tension and circumferential force on the drive drum is proposed to be determined by the formula:

$$S_{\max} = \left[ \sigma_r K_{p_0} - \sigma_u \right] \frac{Bi}{n_0} \quad (60)$$

If the stresses in the belt exceed the fatigue limit, the calculation should be carried out for limited durability, based on the dependencies [15]:

$$\sigma_{\Sigma}^m N = C, \quad (61)$$

where N is the number of loading cycles until the tape is destroyed; - the total stress in the tape from bending, stretching and circumferential force; m and C are coefficients characterizing fatigue properties of the tape.

Endurance calculation makes it possible to avoid premature stratification of belts in conditions of operation, unreasonable excess of diameter of drums and safety margin of belts.

The main reason for the fatigue failure of the belts is the overload of individual gaskets or rubber layers due to the uneven distribution of load between the gaskets.

## References

1. Kovneristov G.B., Tojiyev R.J. Tense state of multilayer conveyor belt. Industrial Transport, Ref.: 2B179,1977

2. Golovan V.P. Study of fatigue wear of conveyor belts during bends on drums and support rollers. Yew. Kiev, 1970.
3. N.V. Erofeeva "Study of cargo segregation on the belt conveyor under the influence of shock pulses" diss.k.t.n. Kemerovo 2011. - 11s.
4. I.V. Galkin, I.V. Shutkin. "Reliability of multilayer rubber-fabric conveyor belts, taking into account the accumulation of damage during impact loads." Yekaterinburg. Mining magazine 2000 No. 1 49-54 s.
5. S.Rjanitsyn A.R. Theory of composite rods of building structures. Stroyizdat, 1948.
6. Pleshkov P.F. theory of calculating wooden composite rods. Gostroyizdat. L. M.,1952.
7. Zolotukhina L.I., Lepetov V.A. Elastic moduli of flat rubber-woven structures during tension and compression. Rubber and Rubber, 1968, No. 10.
8. Bilichenko N.Ya., Vysogin E.M., Zavgorodniy E.K. Operating modes of belt conveyors. Gosttekhizdat. UKRAINIAN SSR.
9. Reshetov D.N. Calculation for the durability of belt gears. "Strength at non-detectable modes of variable stresses," M., ed. AN. USSR, 1954.
10. 10.Chentsov V.F., Golovan V.P., Tojiyev R.J. The design of the experimental bench and the method of strapping conveyor belts to the uterus wear of conveyor belts for fatigue wear. Grabbing structures, healing and calculation of conveyor belts. Abstracts of reports and scientific and technical conference. Sverdlovsk, 1975.
11. 11. Golovan V.P., Tojiyev R.J. Experimental study in the leaching of tag force on delamination. Conveyor belts. "Mining construction and road machines," viz. 23, "Technic," Kiev, 1977